Eur. Phys. J. B **6**, 83–91 (1998)

THE EUROPEAN PHYSICAL JOURNAL B

Azimuthal anchoring of nematic on undulated substrate: Elasticity versus memory

R. Barberi[1], I. Dozov[2,3,a], M. Giocondo[1], M. Iovane[1], Ph. Martinot-Lagarde[2], D. Stoenescu[2,4], and S. Tonchev[3], and L.V. Tsonev[3]

[1] Unità INFM di Cosenza, Dipartimento di Fisica, Università della Calabria, 87036 Rende, Italy
[2] Laboratoire de Physique des Solides, Université Paris-Sud, Bâtiment 510, 91405 Orsay Cedex, France
[3] Institute of Solid State Physics, Bulgarian Academy of Sciences, 72 blvd. Tsarigradsko Chaussee, 1784 Sofia, Bulgaria
[4] INCDFM - Magurele C.P. MG-7, 76900 Bucharest, Romania

Received: 29 April 1998 / Accepted: 23 June 1998

Abstract. We measure the azimuthal anchoring energy of the nematic 5CB on sinusoidal holographic unidimensional and bidimensional gratings. We find that the anchoring strength is almost the same for all of the gratings and up to one order of magnitude stronger than expected by the topographic mechanism proposed by Berreman. We observe strong memory effects which dominate both the elastic anchoring and the easy axis gliding. We show that these memory effects limit from below the anchoring energy and are the main obstacle in the realization of substrates with weak anchoring conditions.

PACS. 61.30.-v Liquid crystals – 61.30.Gd Orientational order of liquid crystals; electric and magnetic field effects on order

1 Introduction

The nematics are anisotropic fluids with long range orientational order: their molecules are in average oriented along the local nematic director $\mathbf{n}$. The scalar order parameter S of the nematic is defined mainly by the thermodynamic conditions and to change its bulk equilibrium value one must apply a very strong external field. On the contrary, the director $\mathbf{n}$ is very sensitive to external fields and to the orientation imposed by the boundaries.

Usually, on contact with a solid substrate the nematic director on the surface $\mathbf{n}_s$ is oriented along some preferred direction $\mathbf{n}_0$, called easy axis. This direction corresponds to a minimum of the anchoring energy $W(\mathbf{n}_s, \mathbf{n}_0)$ (the orientation-dependent part of the nematic-surface interaction energy). In general, W can be very complicated function of the vectors $\mathbf{n}_s$ and $\mathbf{n}_0$, depending on the surface physics and chemistry. For example, on some surfaces two or more easy axes have been observed [1–4], resulting in bistable or multistable nematic orientation. However, in the most of the monostable cases an useful approximation is to separate $W(\mathbf{n}_s, \mathbf{n}_0)$ into two parts, allegedly independent: the zenithal anchoring energy $W_z(\theta_s - \theta_0)$ and the azimuthal one $W_a(\varphi_s - \varphi_0)$, functions respectively only of the zenithal and azimuthal angles of $\mathbf{n}_s$ and $\mathbf{n}_0$. Under this assumption one can study separately W_z and W_a, applying zenithal or azimuthal torques on the surface director $\mathbf{n}_s$.

[a] e-mail: dozov@lps.u-psud.fr

Several different mechanisms have been proposed so far to explain the surface anchoring. The most simple one is just the different chemical composition of the nematic and the substrate. For isotropic flat substrate (or, more generally, for a flat interface between the nematic and an isotropic phase) the normal $\mathbf{N}$ to the surface is a symmetry axis and it should be along an extremum of the zenithal anchoring energy. On the contrary, there is no a particular azimuthal direction in this case and the azimuthal anchoring energy must be strictly zero. In this way the intrinsic anisotropy of the surface can explain the commonly observed homeotropic alignment (with easy axis along $\mathbf{N}$) and the planar or conical degenerated alignment (the anchoring energy maximum is along $\mathbf{N}$, the easy axis is on a cone defined by $\theta_s = const.$).

For an anisotropic substrate there exists also another contribution to the anchoring energy – the anisotropic interactions of the molecules on the two sides of he interface, *e.g.* the anisotropic part of the van der Waals dispersive interactions. In the general case this additional anisotropy breaks the rotational symmetry of the interface around $\mathbf{N}$ and the azimuthal anchoring is no more degenerated: one obtains now monostable or multistable planar or tilted anchorings. This mechanism is probably responsible for the nematic anchoring on anisotropic organic or mineral substrates (stretched or buffed polymers, crystals, *etc.*).

Another mechanism has been proposed long ago by Berreman [5,6] in order to explain the azimuthal

anchoring of mesogens on rubbed isotropic substrates: the anisotropy of the surface topography. On unidirectionally grooved substrate a nematic with planar anchoring is oriented along the grooves, minimizing the bulk elastic energy. The azimuthal anchoring energy obtained in this way varies strongly with the amplitude A and the wavelength Λ of the surface undulation. This "topographic" mechanism of surface alignment can explain the uniform azimuthal anchoring of the nematics on mechanically rubbed mineral [7,8] or organic substrates [8], ruled or holographic gratings [4,9–12], grazing angle SiO evaporated films [13], *etc.*

A large number of experimental studies have confirmed the importance of the alignment mechanisms presented above. However, neither of these mechanisms can explain some commonly observed anchorings, *e.g.* the well known flow alignment of the liquid crystals [10,14,15]: on most of the isotropic or slightly anisotropic solid substrates the nematic anchoring is completely defined by the flow direction during the first contact of the nematic with the surface while filling the sample. Once realized, this anchoring is rapidly memorized and remains for long time, even forever. Moreover, a very strong azimuthal anchoring is obtained in this way. Obviously, the flow alignment cannot be explained by the substrate anisotropy or by the surface topography – it is commonly observed on flat isotropic substrates. Depending on the nature of the surface, two different mechanisms have been proposed to explain the flow alignment and other similar effects. In the case of a "soft" substrate, *e.g.* polymer film, the nematic can induce a strong surface anisotropy [16], for example, by orienting the polymer along the instantaneous local surface director $\mathbf{n}_s$. This orientation is then memorized on the surface and defines eventually the local easy axis. Another possible mechanism, working for both "soft" and "hard" surfaces, is the adsorption of the nematic molecules on the substrate [10]: the adsorbed molecules keep their initial orientation and serve as a new, highly anisotropic substrate. Both these alignment mechanisms are not simple elastic anchorings, but memory effects: under the interaction with the nematic the substrate changes, becomes anisotropic and memorizes the initial surface director field as an easy axis distribution. The anchoring strength (zenithal or azimuthal) of this alignment can be very high – a strong torque must be applied to the surface director in order to deviate it from the easy axis. On longer time scale, however, the anchoring behavior becomes inelastic – under an external torque the easy axis itself rotates slowly to a new direction and remains there after the torque is removed. This easy axis gliding has been recently reported for both lyotropic [17] and thermotropic [18–21] nematics and can be understood as substrate "flowing" or as adsorption-desorption process.

Up to now these memory phenomena have not been studied thoroughly. In fact, for a long time the main interest in nematic alignment has been focused on very strong anchorings. In this case the memory effects are masked by the strong substrate anisotropy and can hardly be observed. The situation changed in the last years, due to the arising interest in weak and moderately strong anchorings. These alignments seem very promising for applications in both nematics [22–24] and ferroelectric C^* smectics [25], *e.g.* to obtain bistable devices by surface anchoring breaking. Several methods have been proposed so far to produce weak anchorings – like using surfaces with small enough intrinsic anisotropy, or substrate topography with small amplitude [4]. However, the experiments have not been very successful so far and for the time being it remains difficult to obtain weak, uniform and stable in the time anchorings. In our opinion the main problem in producing weak anchorings is related to the memory effects – the initial weak surface anisotropy is amplified by the much stronger anisotropy induced on the substrate by the nematic (adsorption or substrate reorientation). The anchoring energy becomes much stronger than expected, but also ill defined due to the memory of the initial state, the orientational hysteresis, the slow gliding of the easy axis, *etc.*

The purpose of this paper is to study quantitatively the importance of the dissipative memory effects, compared to the usual elastic anchoring. We investigate here a simple system – isotropic organic substrate with sinusoidal surface undulation, obtained by photolithography. Several substrates are studied, with different amplitudes of the gratings. Good homogeneous planar orientation of the nematic 5CB is obtained on all of the substrates. The measured azimuthal anchoring energy does not depend on the amplitude of the undulation and is up to one order of magnitude higher than expected by the Berreman's mechanism. At few hours time scale we observe gliding of the easy axis, showing that the anchoring is inelastic, dominated by the memory effects. All of our observations are compatible with initial orientation of the nematic governed by the surface topography and subsequent rapid memorization of the easy axis. The Berreman's effect seems to be important only in the first few seconds; after that the azimuthal anchoring is completely dominated by the memory effects. Our results show that to obtain weak anchoring it is essential to control both the elastic and the memory effects on the surface.

After our experimental work has been already finished and while preparing this paper for publication, we became aware that an independent study, treating also the azimuthal alignment on sinusoidal interferometric gratings, has been recently reported [12]. In our discussion we briefly compare our results with those of Wood *et al.* [12] and we show that the different methods of sample preparation and measurement chosen in the two studies lead to quite different conclusions. We propose an explanation of the reported discrepancies and we show that the two studies are rather complementary than contradictory.

2 Experimental techniques

2.1 Choice of substrates

Our choice of the substrates and of the method to produce the regular surface topography was guided by several requirements. First of all we need isotropic substrates,

in order to exclude the anisotropy of the interactions as a possible source of azimuthal anchoring energy. The surface profile should be simple, easy to produce and to characterize in a repetitive way over a large surface. The profile must be smooth, with wavelength large compared to the nematic correlation length ξ, and without important roughness at ξ-scale. In this way there is no roughness-induced surface order melting, nor large density of surface defects, two phenomena which can appreciably change the expected anchoring strength. Finally, the anchoring energy must be weak or moderately strong (all the existing methods to measure the azimuthal anchoring strength are limited to not too strong energies) and should be varied easily from one substrate to another by simple change of the topography.

To satisfy these requirements we use as anchoring substrates photolithographic gratings with sinusoidal profile, obtained by interferometric exposure of the photoresist. Several gratings were realized by this method, with varying depth of the surface undulation, most of them with simple one-dimensional (1D) surface topography. Two of the gratings were exposed twice, in order to obtain two-dimensional (2D) surface profile (superposition of two sinusoidal waves with orthogonal wave vectors). The gratings were used directly as orienting substrates, *i.e.* the nematic was in contact with the undulated surface of the photoresist.

2.2 Preparation of the gratings

The holographic method used in the present work has been already described in detail [26,27] and here we give only a brief summary of the procedure. Our substrates were glass plates (refractive index $n_g \cong 1.5$ at wavelength $\lambda = 633$ nm) and the photoresist was Shipley AZ-1350 ($n_p = 1.675$ at 442 nm). The similarity of n_g and n_p prevents the formation of a standing wave in the photoresist layer. For the same reason the back surface of the substrate was covered with a black absorbing film. After careful cleaning the plates were pre-baked at 140 °C for two hours to remove the moisture. Immediately after the annealing they were spin coated at 3000 rpm with the photoresist for 20 s through a 0.2 mm Millipore filter in a clean laminar box. Then the plates were baked at 85 °C for 15 min in order to remove the solvent from the resist without complete destruction of the inhibitor.

For small expositions the relation exposure – development is nonlinear. In order to avoid this nonlinearity we started with an uniform non-coherent pre-exposure ($E_p = 50$ mJ/cm^2 from a Hg lamp) and only then we applied the interferometric exposure from an Ar^+ ion laser at $\lambda = 458$ nm. For the 2D gratings two successive exposures were applied, with 90° rotation of the substrate between them. The interferometric exposure was realized by two spatially crossed coherent laser beams with relatively flat wave fronts (intensity of about 5 mW, spatial filters consisting of 25× microscope objectives and 15 μm pinholes).

Table 1. Amplitude of the surface undulation of the gratings and corresponding extrapolation length for the anchoring. The amplitude is measured by AFM and from the optical efficiency of the gratings (the values in the parentheses).

Grating	Amplitude (nm)		Extrapolation length (nm)	
	A_x	A_y	Calculated	Measured
1a	17 (15)	-	5200	280
1b	21 (23)	-	2800	530
1c	38 (46)	-	760	320
1d	45 (52)	-	570	310
1e	46 (58)	-	500	230
2a	10 (13)	10 (13)	∞	490
2b	45 (54)	32 (42)	1240	430

In order to assure conveniently slow developing times (10–40 s) the developer was diluted 1:1 with deionized water. After the development the substrates were rinsed in running deionized water and dried in fresh air by spinning. In our preliminary experiments we observed that the photoresist layer is slowly dissolved in the nematic. To minimize this effect we used an additional stabilizing baking, heating up slowly the plate from room temperature to 110° and keeping it at this temperature for one hour (fast temperature increase or higher baking temperature were avoided because they were observed to destroy the surface topography of the photoresist). After this treatment the solubility of the photoresist decreases and does not disturb the experiment at few hours time scale.

2.3 Measurement of the surface profile

Before the anchoring experiments we characterized the topography of the substrates, measuring the surface profile by two different non-destructive methods. The first one is the measurement of the optical efficiency of the gratings, giving the wavelength Λ and the amplitude A of the surface undulation (Tab. 1), but also confirming indirectly the sinusoidal form of the surface profile.

More direct information about the surface topography of the gratings was obtained by AFM measurements. In Figure 1 we present typical AFM images of the surface undulation for 1D (Fig. 1a) or 2D (Fig. 1b) gratings. For all of the gratings we observe smooth relief with relatively weak roughness at short spatial scale. The surface wave form is approximately sinusoidal for the 1D gratings:

$$z = A_x \sin \frac{2\pi x}{\Lambda} \tag{1}$$

with wavelength $\Lambda = 550$ nm for all of the gratings and with amplitude A varying strongly from one grating

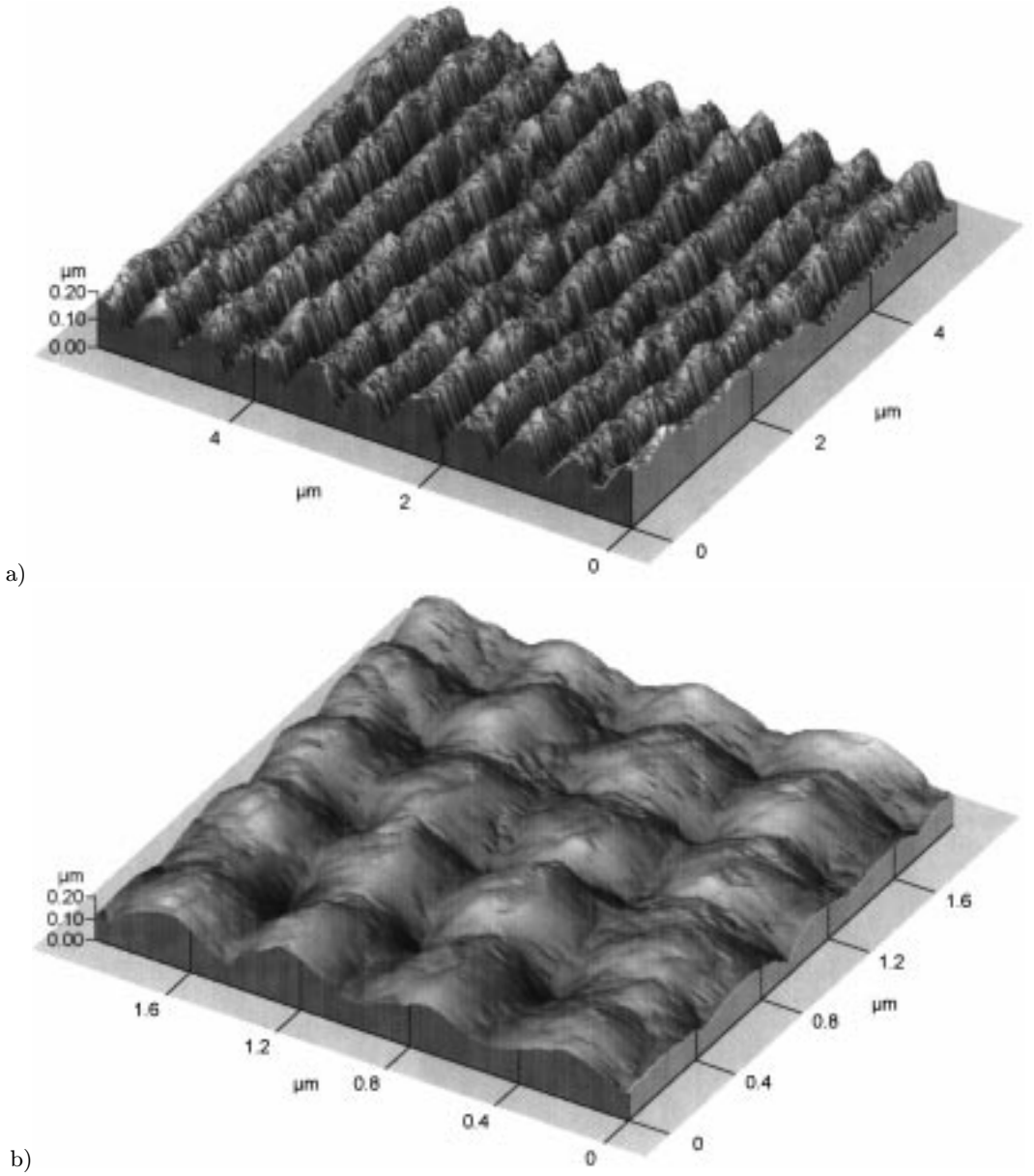

Fig. 1. Surface undulation of the photoresist layer observed by AFM: (a) unidimensional sinusoidal grating 1e; (b) bidimensional grating 2a.

to another, depending on the exposure duration. The amplitudes measured by these two methods (Tab. 1) are in good agreement between them, except for some minor discrepancies, due to the fact that the optical results are averaged over the whole surface of the substrate, while the AFM measures the local profile.

The surface profile of the bidimensional gratings is approximately a superposition of two orthogonal sinusoidal waves (Tab. 1):

$$z = A_x \sin \frac{2\pi x}{\Lambda} + A_y \sin \frac{2\pi y}{\Lambda} \tag{2}$$

with the same wavelength $\Lambda = 550$ nm.

We calculate the expected azimuthal anchoring energy using the Berreman's [5,6] formula under the assumption that the anchoring energy is due only to the surface topography. For simplicity we assume also $K_{11} = K_{22} = K_{33} = K$:

$$W_a = \frac{1}{2} W_{a0} \sin^2(\varphi_s - \varphi_0) \tag{3}$$

where

$$W_{a0} = \frac{1}{2} K A_x^2 \left(\frac{2\pi}{\Lambda}\right)^3 \tag{4}$$

for the unidimensional gratings and

$$W_{a0} = \frac{1}{2} K \left|A_x^2 - A_y^2\right| \left(\frac{2\pi}{\Lambda}\right)^3 \tag{5}$$

for the bidimensional gratings.

In Table 1 we present the extrapolation lengths $L = K/W_{a0}$ calculated using equations (3–5). For the grating 2a we expect almost zero anchoring energy, due to $A_x = A_y$: this grating should be bistable, with two extremely shallow anchoring energy minima along the x and y directions (due to the non-linear terms in the Berreman's energy [4]). All the other gratings are expected to give monostable orientations, with anchoring strength ranging from extremely weak (*e.g.* grating 1a, $L = 5.2$ μm) to moderately weak (*e.g.* grating 1e, $L = 0.5$ μm).

2.4 Measurement of the azimuthal anchoring energy

Several methods have been proposed so far to measure the azimuthal anchoring strength [12,19,20,28–38]. Some of these methods measure directly the anchoring torque [29,30] by torsion pendulum. In the other techniques an external torque (electric [20,32], magnetic [28,31] or mechanical [12,33–38]) is applied on the plate under study and then the deviation $\delta = \varphi_s - \varphi_0$ of the surface director from the easy axis is measured optically from the rotation of the polarization of the transmitted [12,9,20,28,33–38] or reflected [31,32] light. The common limitation of all these techniques is the impossibility to measure strong azimuthal anchoring energie: on one hand it is difficult to apply a field strong enough to broke the anchoring; on the other hand the precision of the optical measurement decreases rapidly with decreasing the extrapolation length.

Here we use a recently developed simple technique, described in detail elsewhere [38]. The nematic is contained between the plate under study (holographic grating) and a standard counter-plate (spherical lens with small curvature). The sample thickness varies from $D = 0$ in the center of the sample up to $D > 30$ μm on the periphery. The local thickness $D(r)$ is calculated as a function of the distance r from the center using the known lens curvature. The surface of the lens is treated to obtain the strongest possible azimuthal anchoring, with extrapolation length supposed to be negligibly small compared to the one on the plate under study. Two different treatments have been used for the lens in the present experiment: SiO evaporation (thickness 15 nm, incidence angle 60°) and rubbed polyimide. In both cases we obtained strong ($L < 40$ nm) and uniform azimuthal anchoring, satisfying our requirements.

The azimuthal torque on the substrate under study is obtained by $\alpha = 90°$ rotation of the lens easy axis relative to the grating easy axis. The bulk torque Γ_b applied on the substrate is a function of the local thickness $D(r)$:

$$\Gamma_b = \frac{K}{D}(\alpha - \delta) \tag{6}$$

and it varies strongly over the cell surface. This enables us to measure the deviation δ as a function of the azimuthal torque. Supposing the anchoring energy W_a to be uniform over the surface (in good agreement with our experimental observations), we obtain $W_a(\delta)$ for deviations δ varying from 0 to 90°.

To measure optically δ we use a simple symmetry property of our uniformly twisted cell [38]: if the sample is rotated under crossed polarizers, the transmission has an extremum when the bisectrix of the polarizers coincide with the bisectrix of the two surface directors (*i.e.* with the director in the middle plane of the cell). This gives us a direct measurement of δ, by rotating the microscope stage with the sample until the minimum transmission is obtained. We do not need to know any material constant of the nematic and the precision of the measurements is limited mainly by the validity of our assumptions: uniformity of the anchoring energy over the surface of the substrate and very strong anchoring on the lens.

3 Experimental results

3.1 Alignment of the nematic 5CB on the gratings

In order to avoid any memory effects related to the filling of the nematic in the cell and to observe the spontaneous easy axis on the substrates, without influence from the neighboring counter-plate, we have taken some special precautions. The sample was placed in a precision mechanical holder which enabled us to increase in large limits the cell thickness ($D > 300$ μm) during the filling. In this way, the elastic torque applied to the substrate by the lens is negligibly small. The hydrodynamic torque, source of flow alignment, is also minimized in this way, but we observed experimentally that in some cases it does not disappear completely. For this reason we filled the samples in the isotropic phase and then decreased slowly the temperature through the nematic–isotropic transition. The spontaneous easy axis reported here has been measured after few minutes of thermalisation at ambient temperature (22 °C), for cell thickness of about 50 μm, large enough to exclude the interaction with the lens. At this large thickness we observe the easy axis directly under a polarizing microscope using simply the rotation of the polarization in the Mauguin's wave-guide regime.

The same procedure was strictly applied while filling all of our samples with the nematic 5CB. Usually, our initial 2×3 cm^2 substrates were cut in four parts and all of them were studied independently in order to check the reproducibility of the alignment and the anchoring strength. Except for some accidental local variations, due to dust particles on the substrates or in the bulk, the reproducibility of the experimental observations was good and in the following we will consider the four parts of the same substrate as being the one and the same cell. For all of the 1D gratings we observed an alignment of the nematic molecules perpendicular to the wave vector of the surface undulation, as expected from the Berreman's aligning mechanism. No exception of this rule has been observed. The same was the case of the anisotropic two-dimensional grating 2b (Tab. 1), where the easy axis was along the lower amplitude wave vector of the grating. For the grating 2a, "isotropic" at lowest order, we observed both of the symmetry allowed easy axes at random. When the cell was thin while filling with the nematic

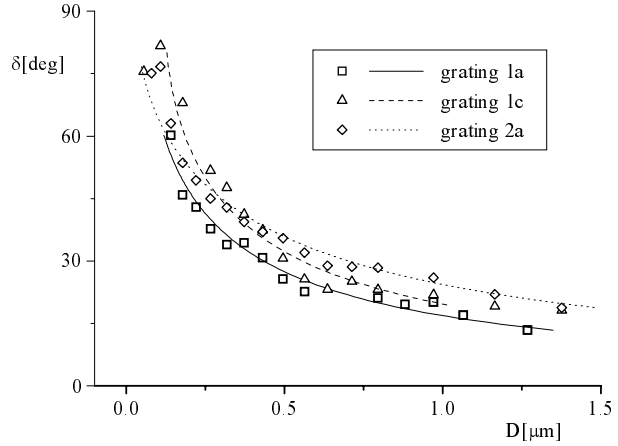

Fig. 2. Elastic deviation δ of the surface director from the easy axis as a function of the local thickness D. The points are the experimental data and the continuous lines are the fits with equation (7).

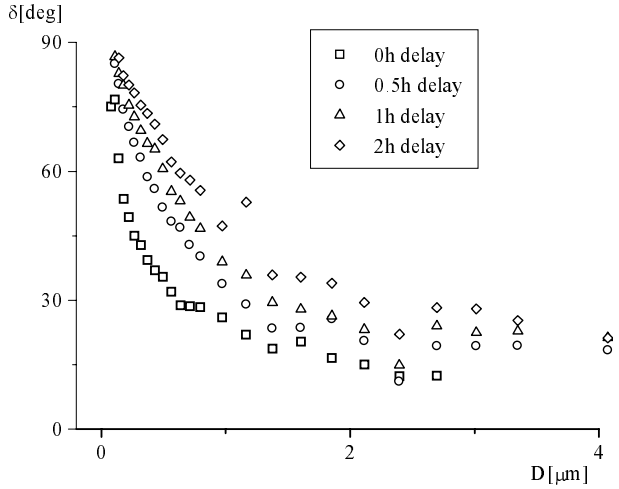

Fig. 3. Gliding of the easy axis for the bidimensional grating 2a. The curve measured immediately after the application of the torque presents the (almost) pure elastic deviation. The curves measured at increasing delay are superposition of the elastic deviation and the increasing easy axis gliding.

($D < 30$ μm) the orientation was usually along the easy axis of the counter-plate.

All these observations are in excellent agreement with the model of Berreman [5,6]: as known for a long time, on isotropic substrates the easy axis of the nematic is completely defined by the surface topography anisotropy.

3.2 Anchoring strength

After the observation of the substrate easy axis we rotate it at approximately 90° relative to the easy axis of the lens. Then we decrease the thickness of the resulting twisted cell until the lens touch gently the substrate in the center of the field of view. Then we measure the local deviation of the surface director on the plate, starting from the center of the sample ($D = 0$) and going all the way to the periphery ($D \geq 30$ μm). The measurement takes about 15 min and it is repeated periodically, in order to detect also the gliding of the easy axis. Some typical results are presented in Figures 2 and 3. As expected, close to the center of the cell, in the thinnest region, the anchoring of the nematic on the substrate is completely broken: the surface torque is too weak and cannot equilibrate the strong bulk torque, transmitted by the twisted nematic. In this central region the cell is untwisted, with director everywhere pointing exactly along the lens easy axis. Farther from the center the bulk torque decreases, resulting in surface director deviation δ smaller than 90°. At high enough thickness ($D \geq 30$ μm) the deviation δ becomes negligibly small.

To obtain the extrapolation lengths for the gratings we fit the data with Rapini-Papoular [39] form of the anchoring torque (*i.e.* anchoring energy given by Eq. (3)):

$$L = (D + D_0)\frac{\sin(2\varphi_s)}{2\varphi_s} \qquad (7)$$

where D_0 is a correction of the thickness D, geometrically defined from the lens curvature: even in the center of the cell the lens and the substrate are not in contact, due to occasional dust particles and/or photoresist layer irregularities. Typically we obtain from the fit $D_0 \sim 300$ nm, in good agreement with the direct measurement of the residual birefringence in the center of the cells.

Surprisingly, for all of the substrates we obtain almost the same extrapolation length $L = 330 \pm 100$ nm, independently from the depth of the surface profile (Tab. 1). This feature is in drastic disagreement with the Berreman's model. The observed values of L are compatible with the extrapolation length expected for the deepest gratings, *e.g.* the grating 1e. It is, however, one order of magnitude shorter than the Berreman's prediction for the low amplitude substrate 1a. Even for the quasi-isotropic bidimensional grating 2a we obtain approximately the same extrapolation length, instead of the expected value $L \gg 10$ μm, corresponding to the extremely weak anchoring energy predicted for this substrate by the model of Berreman.

The above assumption of Rapini-Papoular form of the anchoring energy was made only to simplify the data interpretation when deriving directly the extrapolation length. In reality, our data for $\delta(D)$ enable the determination of the azimuthal torque and anchoring energy as a function of the angle of deviation δ [38]. The results of this analysis are presented in Figure 4 for some of the gratings. For comparison we show also the best fit with the Rapini-Papoular formula, in good agreement with the experimental results (the deviations are due mainly to local defects and irregularities on the surface of the gratings). Once more, this Rapini-Papoular behavior was observed for all of the substrates under study (with almost the same surface anchoring strength for all of them).

For some of the gratings we checked that the curves in Figure 2 are due to an elastic deviation of the surface director $\mathbf{n}_s$ and not to gliding of the easy axis $\mathbf{n}_0$

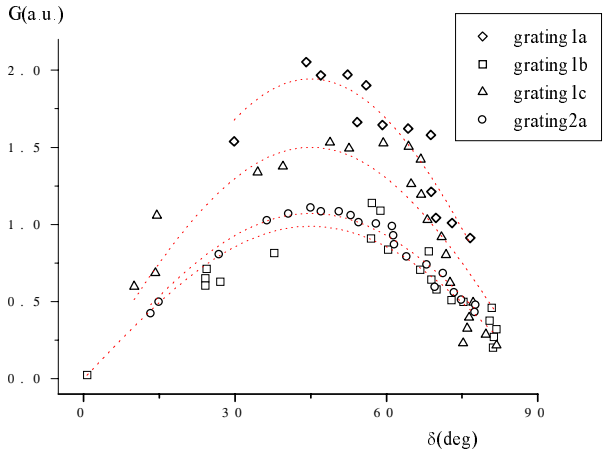

Fig. 4. Surface anchoring torque Γ as a function of the surface angle of deviation δ. The experimental data (points) are fitted with the Rapini-Papoular form of the torque (continuous curves).

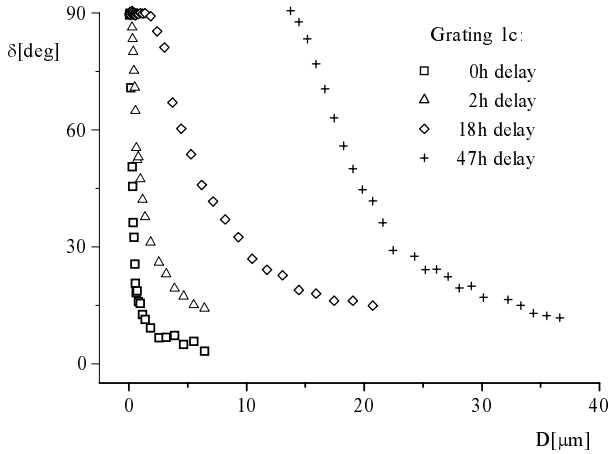

Fig. 5. Long time behavior of the surface orientation.

(see below). For this purpose, after the measurement of $\delta(D)$ we rapidly increase the thickness of the sample up to $D \geq 50$ μm and we verify that $\mathbf{n}_s$ goes everywhere back to its initial orientation, corresponding to $\delta \cong 0$.

3.3 Gliding of the easy axis

When a strong torque is continuously applied for a long time to our substrates, we observe some gliding of the easy axis: not only $\mathbf{n}_s$ deviates from $\mathbf{n}_0$, but the minimum of the surface anchoring energy itself rotates and its orientation becomes a function of the time and the applied torque. This gliding phenomenon has been already reported for both the lyotropic [17] and thermotropic [18–21] liquid crystals. Two possible mechanisms has been proposed so far to explain the gliding: the adsorption-desorption of the nematic molecules on the substrate or the reorientation of the molecules of the substrate itself under the torque applied by the liquid crystal.

Our data for the gliding are less reproducible from one grating to another than the corresponding anchoring strength data. They are strongly influenced by the finite solubility of the photoresist material in the 5CB. Although after the "stabilization" of the photoresist by baking of the grating we observe a decreasing of the solubility, it does not disappear completely. Typically, 10 hours after filling the sample we observe in the thinner region of the cell a decreasing of the clearing temperature of the nematic, due to the high concentration of the dissolved photoresist there. This leads to weaker anchoring and faster gliding of the easy axis. In about 24 hours at room temperature we observe in the center of the cell transition to the isotropic phase and our measurements are no more meaningful.

The typical results for the long-time evolution of the anchoring are presented in Figure 5 for the grating 1c. The first curve is measured immediately after the filling of the sample and represents the purely elastic deviation of the surface director from the initial easy axis. The second and the third curves are measured respectively after 2 and 18 hours delay. They are a superposition of the elastic deviation and the anchoring gliding. Finally, the last curve is taken after 47 hours and is seriously influenced by the solubility of the photoresist. For this curve the bulk properties of the nematic vary appreciably over the surface of the sample, due to the local variations of the photoresist concentration. Up to $D \approx 14$ μm the 5CB is in the isotropic phase and δ has no sense. For higher thickness the deviation is due mainly to the anchoring gliding and to the memory effects and not to the elastic anchoring energy.

4 Discussion and conclusion

The memory phenomena, related to the nematic alignment, have been already studied before [10,15,6,19,40–44]. The memorization of the initial orientation, obtained by flow alignment or under external field, has been reported on various substrates: rubbed or unrubbed polymers [16,19,40,42,43], bare glass or ITO [41,44], normally or obliquely evaporated SiO layers [15,41]. The memory phenomena has been discussed also for undulated substrates [10,12,19], leading to quite contradictory conclusions. For example, in the case of nematic alignment on photolitographic gratings Cheng and Boyd [10] found that "grooves are neither necessary nor sufficient to produce alignment" and that the anchoring is due mainly to the interfacial forces memorized on the surface during the first appearance of the nematic order in the sample. On the other hand, Wood *et al.* [12] reported recently good agreement between the model of Berreman and the anchoring energy measured on sinusoidal gratings.

These discrepancies are easy to understand. The measurement of the azimuthal anchoring strength is relatively difficult problem and most of the studies are just qualitative. Also, the neat separation of the elastic anchoring from the easy axis gliding and hysteresis is impossible for most of the measurement methods. By our knowledge, here we present the first quantitative measurements separating and comparing the strength of the Berreman's

elastic energy and the *memory of the anchoring* on the surface. This is achieved mainly by an appropriate choice of our substrates. The regular, large wave length profile of our gratings is easy to characterize, leading to precise estimation of the Berreman's elastic contribution. The total anchoring energy observed on our plates is weak enough to be reliably measured by the existing experimental techniques, but it remains still up to one order of magnitude stronger than the "topographic" contribution alone. When we fill our samples with precaution, in order to avoid any parasitic alignment effects, due to the flow and to the bulk elasticity, we obtain an uniform orientation of the nematic over the whole substrate area. The observed spontaneous easy axis is always along the deepest valleys on the grating, in agreement with the Berreman's model. The exception which confirms this rule is the quasi-isotropic grating 2a, for which the easy axis on the substrate depends on the lens orientation even for very thick samples ($D \sim 30$ μm).

Taking into account that our photoresist is strictly isotropic (we have verified experimentally that there is no photoalignment due to the exposition to polarized laser light during the grating fabrication), we conclude that the spontaneous orientation is due to the surface topography. However, this is the only indication in our observations of the existence of the surface profile induced alignment. Indeed, our measurements show that the total elastic anchoring energy on our gratings is much stronger than the expected topographic contribution and does not depend on the amplitude of the surface undulation. Obviously, once selected, the spontaneous easy axis is memorized on the surface and then the Berreman's contribution is overwhelmed by the much stronger contribution of the memory effect.

For the time being the mechanism of the memory is not clear. For "soft" substrates, as our photoresist layer, one can imagine [16] that the nearby nematic induces order on the substrate, reorienting its molecules. The newly anisotropic substrate then orients in its turn the nematic along the direction initially "imprinted" on it. During the process of memorization there is no torque applied by the nematic – the order is created in the substrate along the instantaneous surface director. Once ordered, the layer molecules can rotate only collectively. Due to the steric hindrance and to the solid friction in the substrate this reorientation is very difficult: now the aligning layer can support or can apply large torques without further change.

The second mechanism proposed so far to explain the anchoring memory is the adsorption of an oriented nematic layer on the substrate. This creates a "new" stiff and highly anisotropic substrate, on which is anchored the bulk liquid crystal. Once more, the collective reorientation of the adsorbed layer is impossible and it can support high torques. At longer time scale this layer can be slowly reoriented by continuous desorption and re-adsorption of individual nematic molecules.

Both these mechanisms are compatible with our experimental data and here we will not try to guess which one of them is in reality responsible for the observed behavior. We note, however, that in both cases the anchoring strength is limited from below by the physical and chemical properties of the substrate and by its interactions with the nematic, and not by the surface profile. Similar behavior was observed recently also for the 5CB anchoring on flat anisotropic alignment layers [21]. We conclude that the memory effects are the main difficulty in the fabrication of uniform, but weak azimuthal anchorings: even if the bulk or surface anisotropy of the substrate is very low, the orientational memory on the alignment layer can lead to a very strong anchoring energies. Obviously, for the practical realization of weak anchorings more attention must be paid to the chemical composition of the substrates (and, maybe, of the nematic itself), than to the physical treatments by which the surface anisotropy is created. We expect that the same difficulty to obtain weak azimuthal anchorings will be present also when the weak substrate anisotropy is obtained by other means – *e.g.* by gentle rubbing or buffing, by weak photoalignment, *etc.*

In principle, the information about the memory mechanism is contained in the long time behavior of the anchoring, especially in the time dependence of the easy axis gliding. In our case the interpretation of this behavior is quite difficult, due to the solubility of the photoresist in the nematic. We clearly observe gliding of the anchoring, but it is accompanied with change of the anchoring strength and even with a variation of the bulk properties of the mesogen, *e.g.* the clearing temperature. Obviously, our system is too complicated and cannot be used for the study of the memory mechanism.

We can now briefly compare our results and conclusions with those recently presented by Wood *et al.* [12] for the azimuthal anchoring energy of the nematic mixture E7 on Shipley S1805 photoresist based holographic gratings. This nematic-substrate system is very similar to the one presented here and we expect qualitatively the same behavior in both cases. However, at first glance, the results in reference [12] disagree with our observations: the anchoring energy measured by Wood *et al.* is in excellent agreement with the model of Berreman, at least when the expected extrapolation length is smaller than 10 μm. To understand this discrepancy we need to compare also the experimental measurement techniques used in both studies. In our case the sample is filled while in isotropic state and cooled down under almost no torque ($D > 300$ μm). Then the thickness is decreased and the deviation δ is measured as a function of D under large applied torques (0.1 μm $< D < 30$ μm). This enables us to separate the elastic anchoring from the memory effects and from the slow evolution of the orientation (anchoring gliding). We can also directly separate these effects by continuous variation of the local sample thickness during the experiment. On the contrary, in reference [12] the thickness is constant for each sample (5 μm $< D < 15$ μm). The cells are filled in the isotropic phase and then cooled down to room temperature for the measurement of the deviation δ (the torque remains almost the same during the cooling). It is impossible in this case to separate the elastic and the memory effects: if the orientation on the substrate is memorized during the transition to the nematic state,

then δ remains unchanged on cooling and is defined just by the equilibrium between the bulk torque and the Berreman's topographic effect at the clearing temperature T_c. This scenario explains the remarkable agreement of the measured deviations with the model of Berreman when the values of the elastic constants corresponding to T_c are used [12]. In our opinion, the results of Wood *et al.* confirm indirectly our conclusions: the Berreman's alignment mechanism is important only to define the initial orientation of the easy axis; the anchoring energy corresponding to this axis is dominated by the memory effects, in our case much stronger than the topographic alignment.

In conclusion, we studied the azimuthal anchoring energy of the nematic 5CB on sinusoidal holographic unidimensional and bidimensional gratings. The measured anchoring strength is almost the same for all of the gratings and up to one order of magnitude stronger than expected by the topographic mechanism proposed by Berreman. We observe strong memory effects which dominate both the elastic anchoring and the easy axis gliding. The orientational memory of the substrate seems to be defined mainly by the chemical composition of the surface. We show that these memory effects limit from below the anchoring energy and are the main obstacle in the realization of substrates with weak anchoring conditions.

This work was supported by Grant IC 15 CT 96 0744 from the Copernicus Program of the European Community and by grant n°582 from the Ministry of Education, Science and Technology of Bulgaria.

References

1. P. Grandjean, Bull. Soc. Fr. Mineral. **39**, 164 (1916).
2. M. Monkade, M. Boix, G. Durand, Europhys. Lett. **5**, 697 (1988).
3. B. Jerome, P. Pieranski, M. Boix, Europhys. Lett. **5**, 693 (1988).
4. G.P. Bryan-Brown, M.J. Towler, M.S. Bancroft, D.G. McDonnell, SID94 Digest, 209, (1994).
5. D.W. Berreman, Phys. Rev. Lett. **28**, 1683 (1972).
6. D.W. Berreman, Mol. Cryst. Liq. Cryst. **23**, 215 (1973).
7. C. Mauguin, Bull. Soc. Fr. Mineral. **34**, 71 (1911).
8. U. Wolf, W. Greubel, H. Krüger, Mol. Cryst. Liq. Cryst. **23**, 187 (1973).
9. D.C. Flanders, D.C. Shaver, H.I. Smith, Appl. Phys. Lett. **32**, 597 (1978).
10. J. Cheng, G.D. Boyd, Appl. Phys. Lett. **35**, 444 (1979).
11. M. Nakamura, M. Ura, J. Appl. Phys. **52**, 210 (1981).
12. E.L. Wood, G.W. Bradberry, P.S. Cann, J.R. Sambles, J. Appl. Phys. **82**, 2483 (1997).
13. E. Guyon, P. Pieranski, M. Boix, Lett. Appl. & Eng. Sci. **1**, 19 (1973).
14. B. Jerome, P. Pieranski, J. Phys. France **49**, 1601 (1988).
15. H. Yokoyama, S. Kobayashi, H. Kamei, J. Appl. Phys. **56**, 2645 (1984).
16. N.A. Clark, Phys. Rev. Lett. **55**, 292 (1985).
17. E.A. Oliveira, A.M. Figueiredo Neto, G. Durand, Phys. Rev. A **44**, R825 (1991).
18. T. Nose, S. Masuda, S. Sato, Jpn J. Appl. Phys. **1** 30, 3450 (1991).
19. Y. Sato, K. Sato, T. Ushida, Jpn J. Appl. Phys. **31**, L579 (1992).
20. V.P. Vorflusev, H.-S. Kitzerow, V.G. Chigrinov, Appl. Phys. Lett. **70**, 3359 (1997).
21. D. Stoenescu, *et al.*, to be published.
22. R. Barberi, G. Durand, Appl. Phys. Lett. **58**, 2907 (1991).
23. R. Barberi, M. Giocondo, G. Durand, Appl. Phys. Lett. **60**, 1085 (1992).
24. I. Dozov, M. Nobili, G. Durand, Appl. Phys. Lett. **70**, 1179 (1997).
25. N.A. Clark, S.T. Lagerwall, Appl. Phys. Lett. **36**, 899 (1980).
26. L. Mashev, S. Tonchev, Appl. Phys. A **26**, 143 (1981).
27. L. Mashev, S. Tonchev, Appl. Phys. B **28**, 349 (1982).
28. J. Sicart, J. Phys. Lett. **37**, L-25 (1976).
29. S. Faetti, M. Gatti, V. Palleschi, T.J. Sluckin, Phys. Rev. Lett. **55**, 1681 (1985).
30. S. Faetti, V. Palleschi, Liq. Cryst. **2**, 261 (1987).
31. S. Faetti, M. Gatti, V. Palleschi, A. Schirone, Il Nuovo Cim. D **10**, 1313 (1988).
32. S. Faetti, M. Nobili, A. Schirone, Liq. Cryst. **10**, 95 (1991).
33. V. Sergan, G. Durand, Liq. Cryst. **18**, 171 (1995).
34. S. Faetti, M. Nobili, Physics Lett. A **217**, 133 (1996).
35. V.P. Vorflusev, H.-S. Kitzerow, V.G. Chigrinov, Jpn J. Appl. Phys. **34**, L-1137 (1995).
36. T. Akahane, H. Kaneko, M. Kimura, Jpn J. Appl. Phys. **35**, 4434 (1996).
37. V.P. Vorflusev, H.-S. Kitzerow, V.G. Chigrinov, Appl. Phys. A **64**, 615 (1997).
38. E. Polossat, I. Dozov, Mol. Cryst. Liq. Cryst. **282**, 223 (1996).
39. A. Rapini, M. Papoular, J. Phys. Coll. **30**, C4-54 (1969).
40. N. Koshida, S. Kikui, Appl. Phys . Lett. **40**, 541 (1982).
41. H.A. van Sprang, Mol. Cryst. Liq. Cryst. **97**, 255 (1983).
42. Y. Ouchi, M.B. Feller, T. Moses, Y.R. Shen, Phys. Rev. Lett. **68**, 3040 (1992).
43. B.O. Myrvold, Liq. Cryst. **18**, 287 (1995).
44. L.V. Tsonev, M.P. Petrov, G. Barbero, submitted to Liq. Cryst.